

We are IntechOpen, the world's leading publisher of Open Access books Built by scientists, for scientists

6,900

Open access books available

185,000

International authors and editors

200M

Downloads

Our authors are among the

154

Countries delivered to

TOP 1%

most cited scientists

12.2%

Contributors from top 500 universities



WEB OF SCIENCE™

Selection of our books indexed in the Book Citation Index
in Web of Science™ Core Collection (BKCI)

Interested in publishing with us?
Contact book.department@intechopen.com

Numbers displayed above are based on latest data collected.
For more information visit www.intechopen.com



Crystallographic Observation and Delamination Damage Analyses for Thermal Barrier Coatings Under Thermal Exposure

Kazunari Fujiyama
Meijo University,
Japan

1. Introduction

Recently, as the service condition of high temperature components are becoming severer and almost beyond its ultimate performance, protective coatings are expected to be effective solutions to keep the reliability and durability of high efficiency apparatus. Thermal barrier coatings(TBCs) have been applied to cool down the metal temperature and to protect damage under thermal exposure of hot gas path components in gas turbines[1]. As TBCs are used in very severe conditions, thermally induced damage and material degradation are inevitably induced during service and delamination of coating layer may occur finally as the result of coalescing multiple lateral cracks and some vertical cracks after the evolution of oxide layer between top coat and bond coat schematically shown in Fig.1.

However, the mechanism of damage and degradation is still not clear enough because there are so many factors affecting the delamination life[2]. Therefore, one objective of this paper is to focus on how the EBSD observation of thermal exposure samples of TBC top coatings can be applied to identify the particle morphologies after the plasma spraying and another is to evaluate the damage process until the delamination of top coatings.

Optical microscope observation was conducted on laboratory test samples of TBC system after thermal exposure using electric furnace and for measuring the pore fraction amounts during the process. SEM observation was also conducted to measure cracks induced by thermal exposure. It should be noted that the detailed microstructural features of TBC top coat have not been clearly observed by the conventional optical microscope or scanning electron microscope (SEM) because those measures cannot reveal the detailed proper boundaries of top coat splat particles. Electron backscatter diffraction (EBSD) method[3][4] is expected to be an effective tool for observing the morphologies of such particles, but the application of EBSD to the TBCs has not been popularized enough due to the difficulties in preparing the observation surface of TBCs and in identifying the exact crystal systems. We demonstrate the current status for visualizing the splat morphologies in top coat by EBSD and depict some problems in applying the technique. EDS(Energy Dispersive Spectroscopy)

analyses and indentation tests are also used as the tools for investigating the sintering of top coatings and the evolution of TGO(Thermally Grown Oxide) layers. Finally this article presents some evaluation diagram for the top coat delamination based on the obtained experimental results.

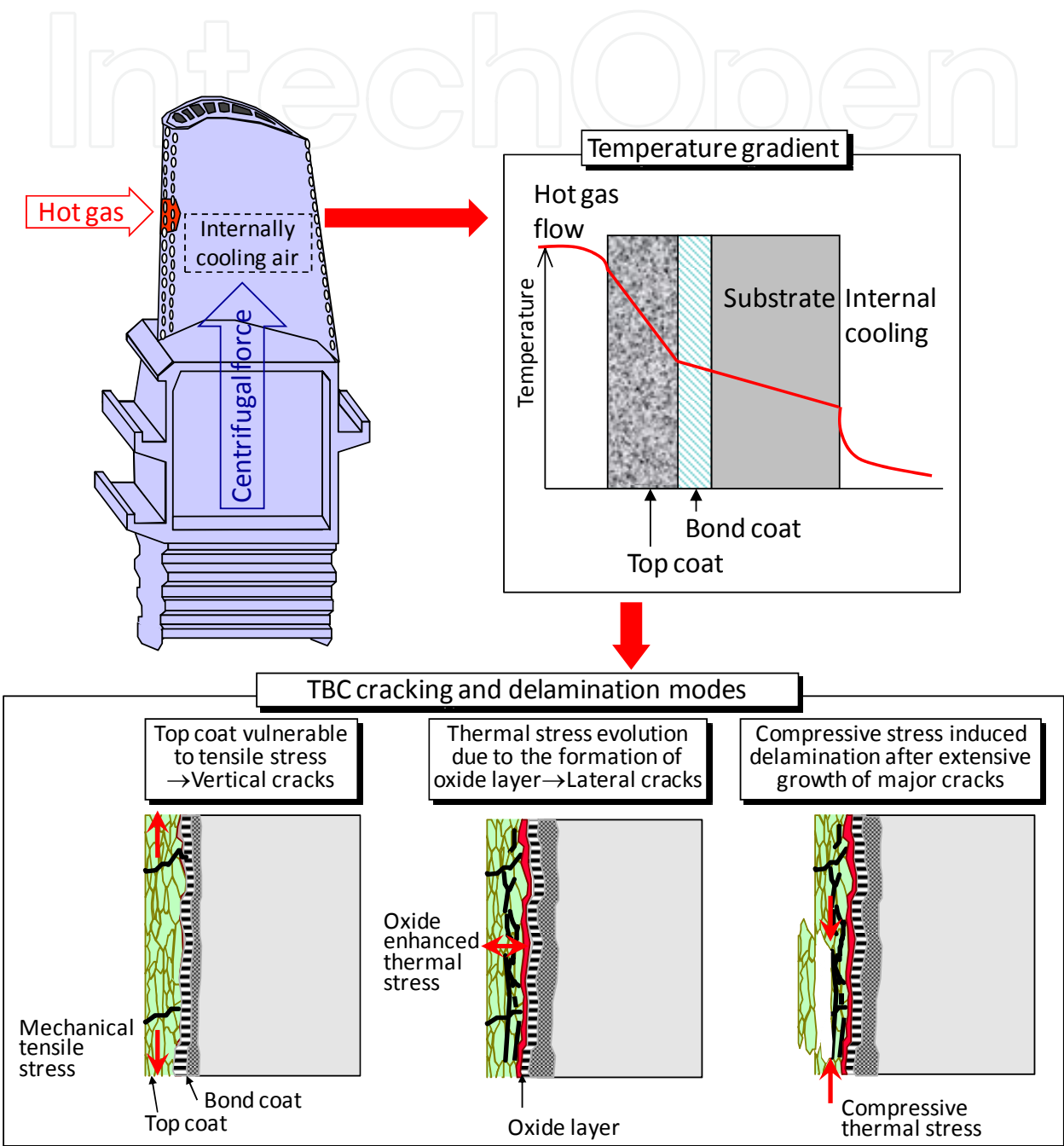
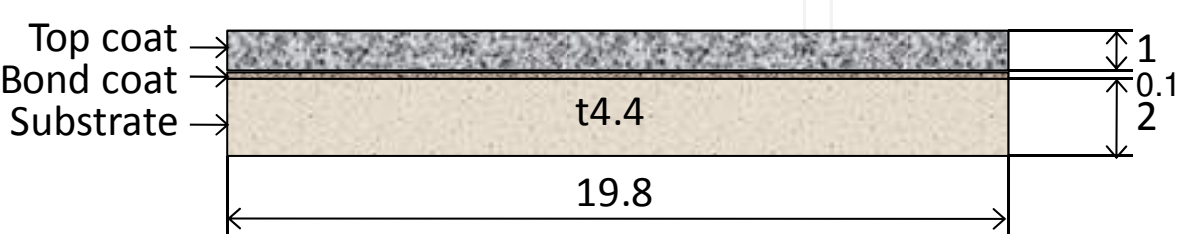


Fig. 1. Schematic illustration for the delamination of TBC in gas turbine blade under temperature gradient.

2. Specimen preparation [5]

Atmospheric plasma sprayed ceramic coatings are widely used as the thermal barrier coating (TBC) in high temperature components typically in gas turbine hot gas path sections. The TBC samples tested here are consisted with three layers: top coat, bond coat and substrate as shown in Fig.2. The top coat is consisted with Yttria- Partially Stabilized Zirconia(PSZ). The thickness of top coat region is 1mm, considerably thicker compared with the commercial TBC system in actual gas turbines.



Top coat : 8wt% Y₂O₃-ZrO₂(1mm thick); APS(Atmospheric Plasma Spraying)
Bond coat : CoNiCrAlY(100µm thick); LPPS(Low Pressure Plasma Spraying)
Substrate : MA263(2mm thick)

Fig. 2. TBC specimen geometry.

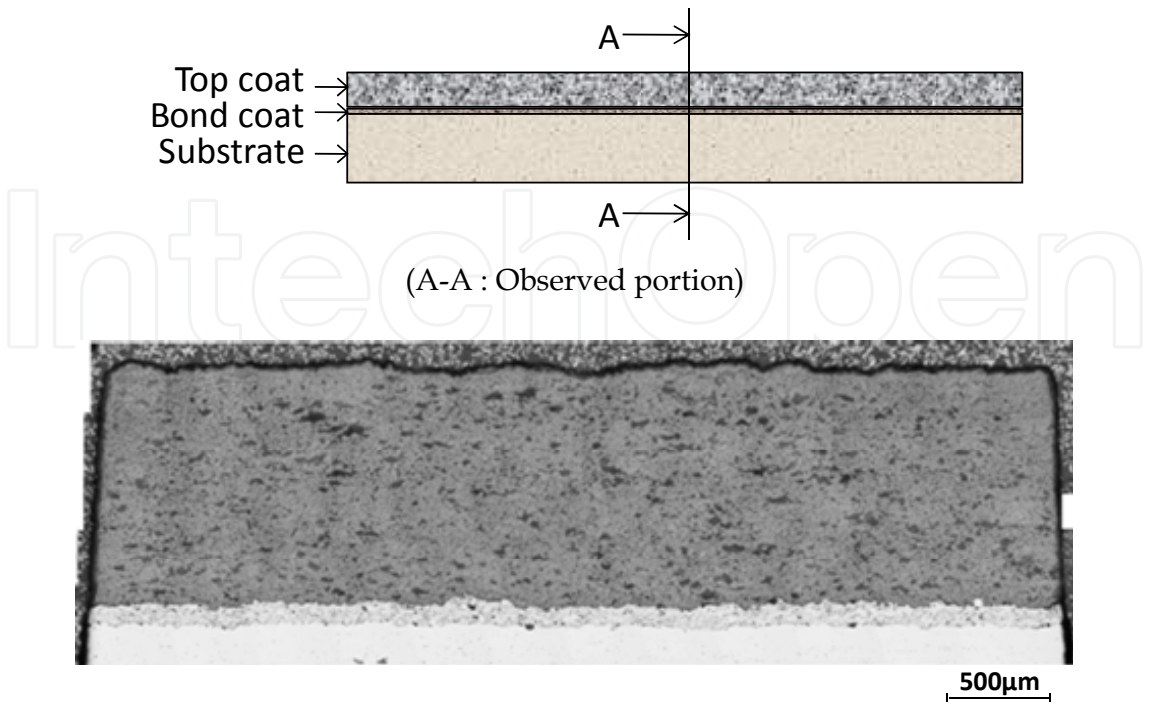
Thermal exposure tests were conducted up to 1000 hours under constant temperature conditions at 900°C and at 1000°C using an electric furnace up to 1000hrs. The specimens were cut into observation samples with the surface finished with colloidal alumina with particle diameters as 0.1 to 3 micron meters.

3. Optical microscope observation and measurement of pores and cracks [5]

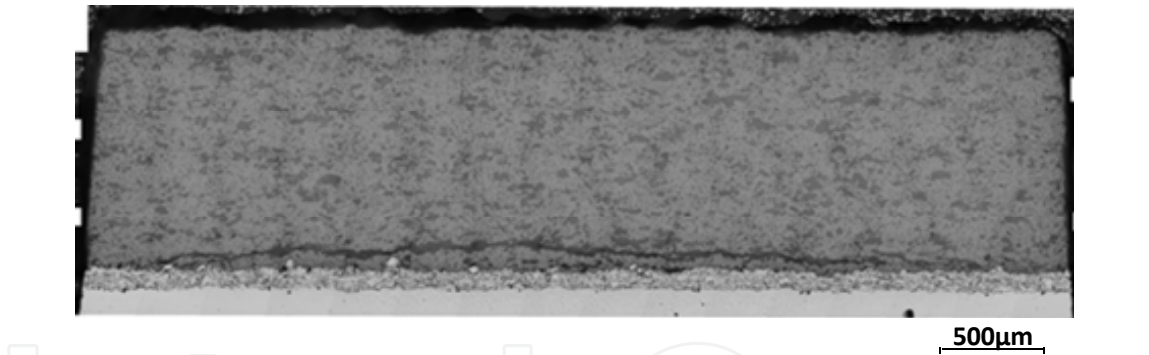
Figure 3 shows the delamination process exposed at 900°C. Macro cracks grow laterally in the top coat just above the bond coat. The surface macro crack is located at the interface between top coating and bond coat besides at the mid section crack is located above the bond coat within top coat. Fig.4 shows the cross section exposed for 50hours at1000°C. The delamination was clearly found in this case.

Figure 5 shows optical microscope observation of top coat at the region near the bond coat. Reduction of the area by pores was observed for samples after thermal exposure compared with as-sprayed samples despite of the non-monotonic trend with exposure time. Fig.6 shows the traced pore image for image processing based on optical microscope photos. Area fractions of pores were obtained from the area ratio of pores (black area) to the observed area.

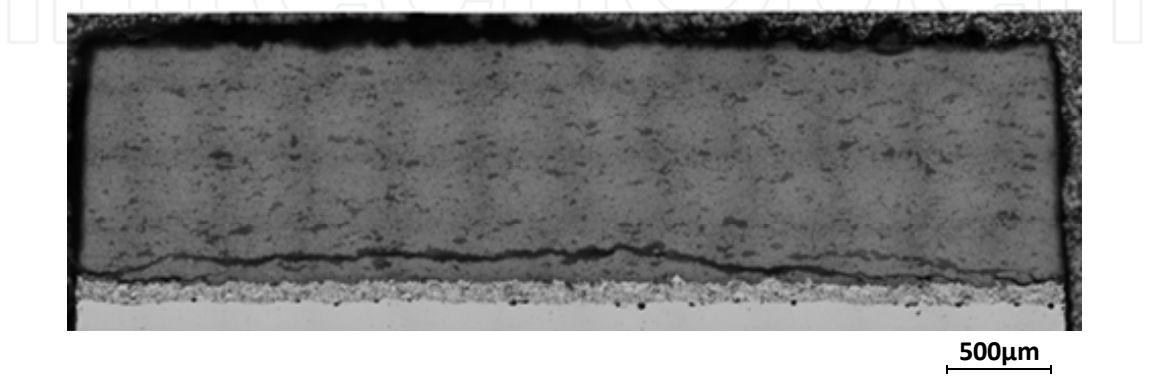
Figure 7 shows the trend of area fraction of pores against thermal exposure time. Reduction in area fraction of pores was observed at the initial stage of heating but the decreasing trend was not monotonic. The area fraction of pores showed similar levels exposed at 900°C for 500h and at 1000°C for 75h.



(a)As sprayed



(b)900°C 100h



(c)900°C 300h

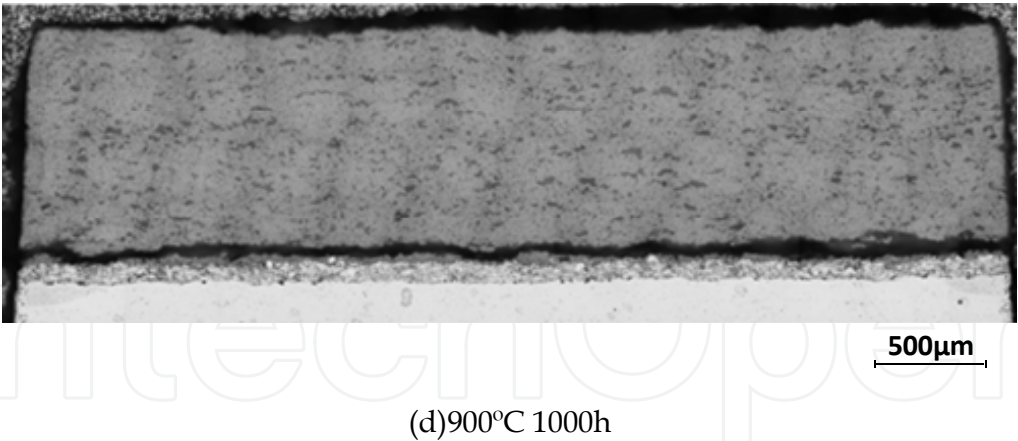


Fig. 3. Optical microscope observation of the cross section at 900 °C exposure tests.

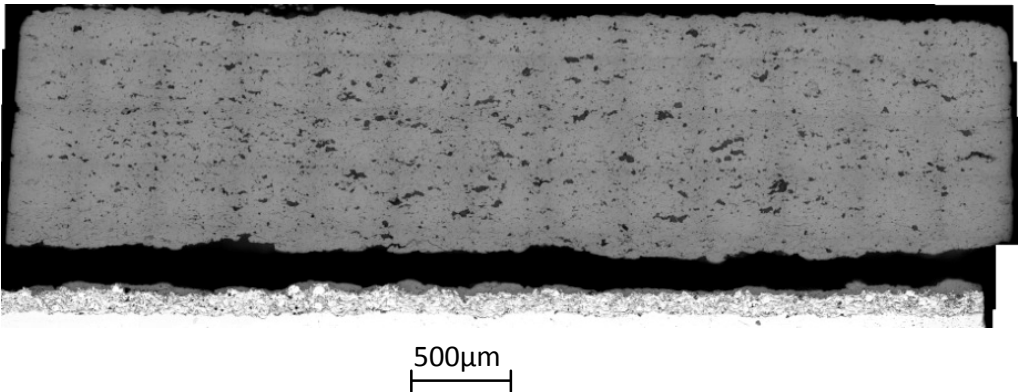


Fig. 4. Optical microscope observation of the cross section at 1000 °C-50h exposure test.

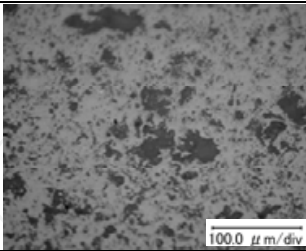
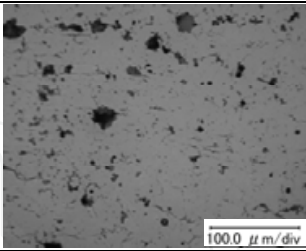
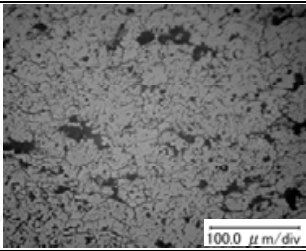
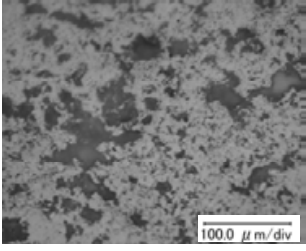
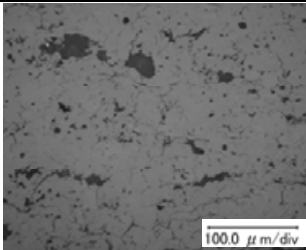
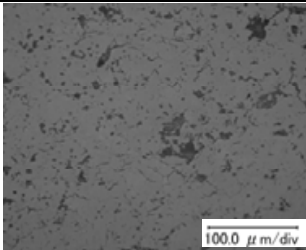
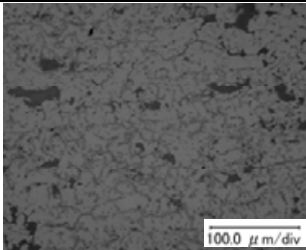
As sprayed	Exposure hours at 900 °C		
	100	500	1000
			
	Exposure hours at 1000 °C		
	50	75	100
			

Fig. 5. Optical microscope observation of top coat.

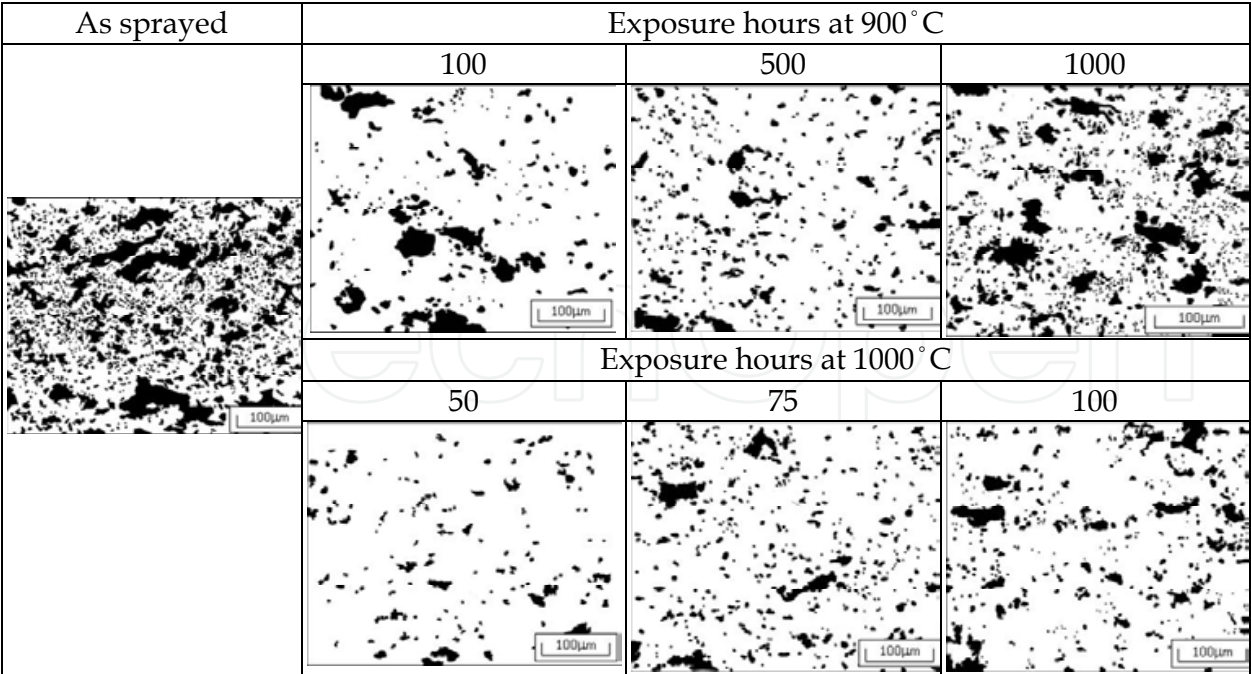


Fig. 6. Pore area trace of optical microscope image in top coat.

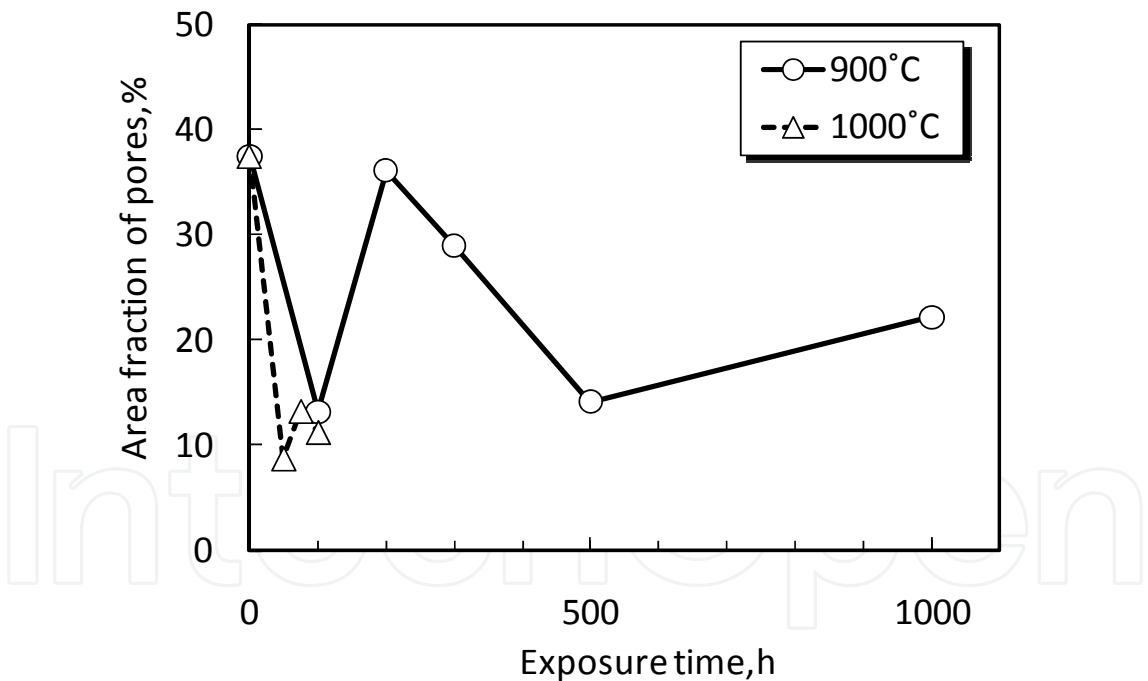


Fig. 7. The trend of area fraction of pores in top coat against exposure time.

4. SEM/EBSD observation and measurement of crack growth trend [5]

SEM observation was conducted using the thermal field-emission scanning electron microscope mainly used for investigating crack morphologies. Observed cracks were traced manually and then processed by image processing software to measure crack length. TGO layer was investigated using EDS system of SEM to identify the elements of oxides.

EBSD observation was conducted using Tex SEM Laboratory OIM 4.6 system attached to the SEM. IPF(Inverse Pole Figure) maps were obtained from the position adjacent to the bond coat within top coat(bottom region), middle of top coat thickness(middle region) and near surface region of top coat(top region). The tentative crystal system for EBSD observation was ZrO_2 cubic system because of the easiness of observation of particle morphologies though PSZ has commonly tetragonal system. It should be noted that the EBSD equipment has the limitations to characterizing the tetragonal system from the cubic system for the subject top coating PSZ, requiring further development of the technique to identify the tetragonal system clearly and easily.

Figure 8 shows the matching of SEM image and EBSD IPF maps near bond coat for as-sprayed samples. The splat particle morphologies were clearly observed by IPF maps, which cannot be obtained from the SEM image. The splat morphologies are classified into two typical groups. One is large granular type particles which might not be melted completely at the spraying process, and the other is the cluster of small columnar particles which might be formed by crystallization from completely melted particles. Cracks are found to be affected by splat microstructures after crystallization completed.

Figure 9 shows the matching of SEM image and IPF maps from bottom to top region of top coat for samples exposed at 900°C for 500h. Though there is no significant difference in crystallographic features and crack morphologies in test samples and locations, subsequent crack growth and reduction of pores can be seen by comparing with as-sprayed sample shown in Fig.8.

Figure 10 shows the matching of SEM image and IPF maps near delamination portion samples for $1000^\circ\text{C}/500\text{h}$ exposed sample. Larger cracks can be found by comparing with Figs.8 and 9.

Figure 11 shows IPF maps at higher magnification for typical crack morphologies. There are three major cracking patterns. The first is the interface cracking between large granular particles and the cluster of small columnar particles, the second is the interface cracking along larger granular particles which is often perpendicular to thickness direction of coating and the third is the transgranular cracking across the cluster of small columnar particles. The cracking orientation seems almost perpendicular to crystal growth direction at the columnar small particle regions. Those cracks are thought to be introduced during cooling process after crystallization was completed. For heated samples cracks are thought to grow from initially introduced cracks during spraying process and increasing in number at successive exposure test. There is no apparent dependence of crack morphologies on the position toward the thickness direction of top coat.

Figure 12 shows the comparison of IPF maps before and after indentation tests for as-sprayed sample. Indentation tests were conducted by 500mN load. Cracks or pores were emanated from the corner of the diamond shaped indentation and showed the apparent tendency that cracks developed along the intergranular path along relatively larger splat particles and the extensive drop out occurred at the small particle zones. This result suggested the very low resistance at small particle (or amorphous) zones and particle boundaries but relatively higher resistance at larger particles. Fig.13 shows the local zoomed up IPF maps with SEM image of green circle region in Fig.12 before and after indentation test. This map clearly indicated the transgranular cracking path from the indentation corner and coalesced with the pre-existing crack across relatively large particles.

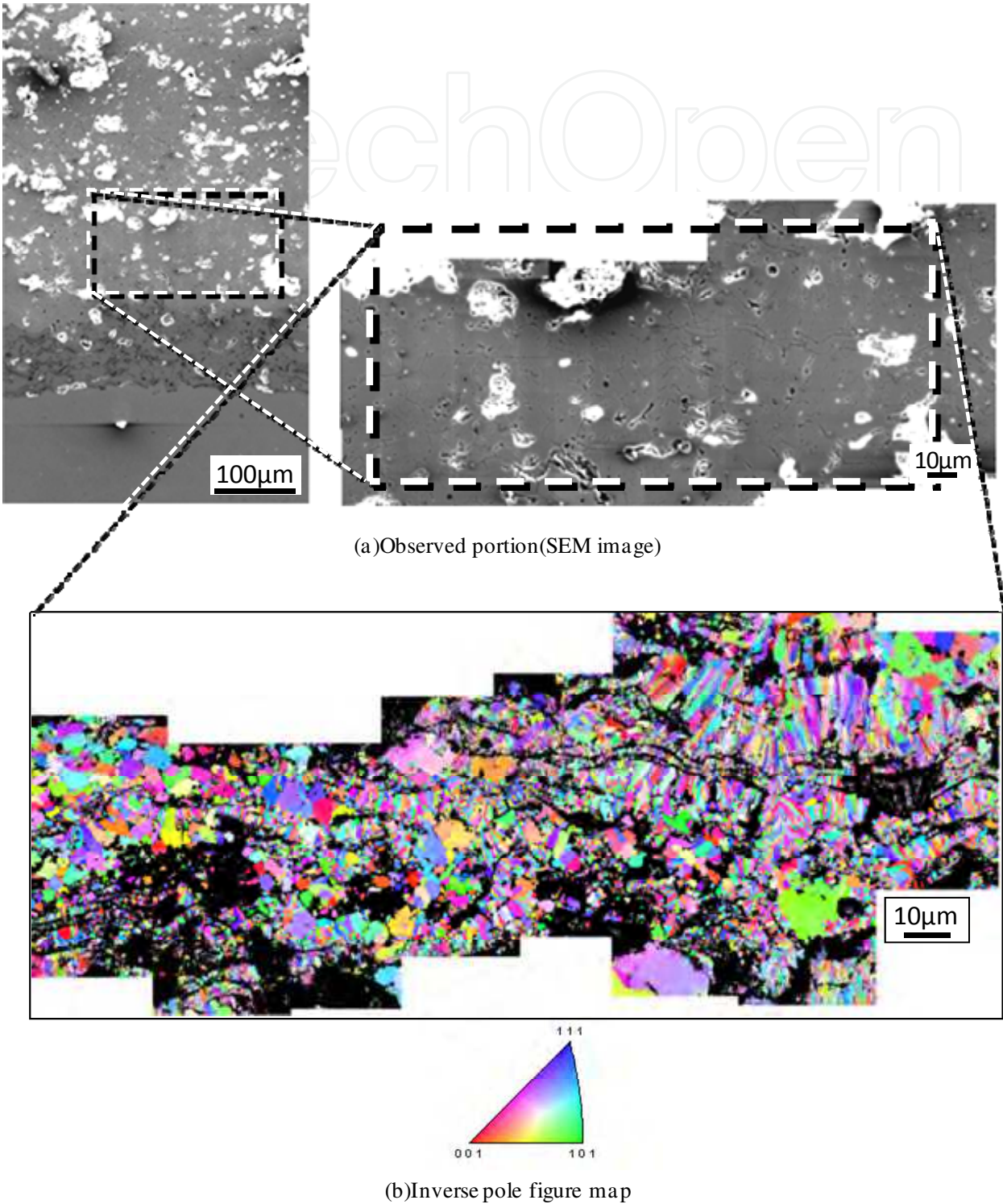


Fig. 8. Matching of SEM observations and IPF map of as-sprayed sample.

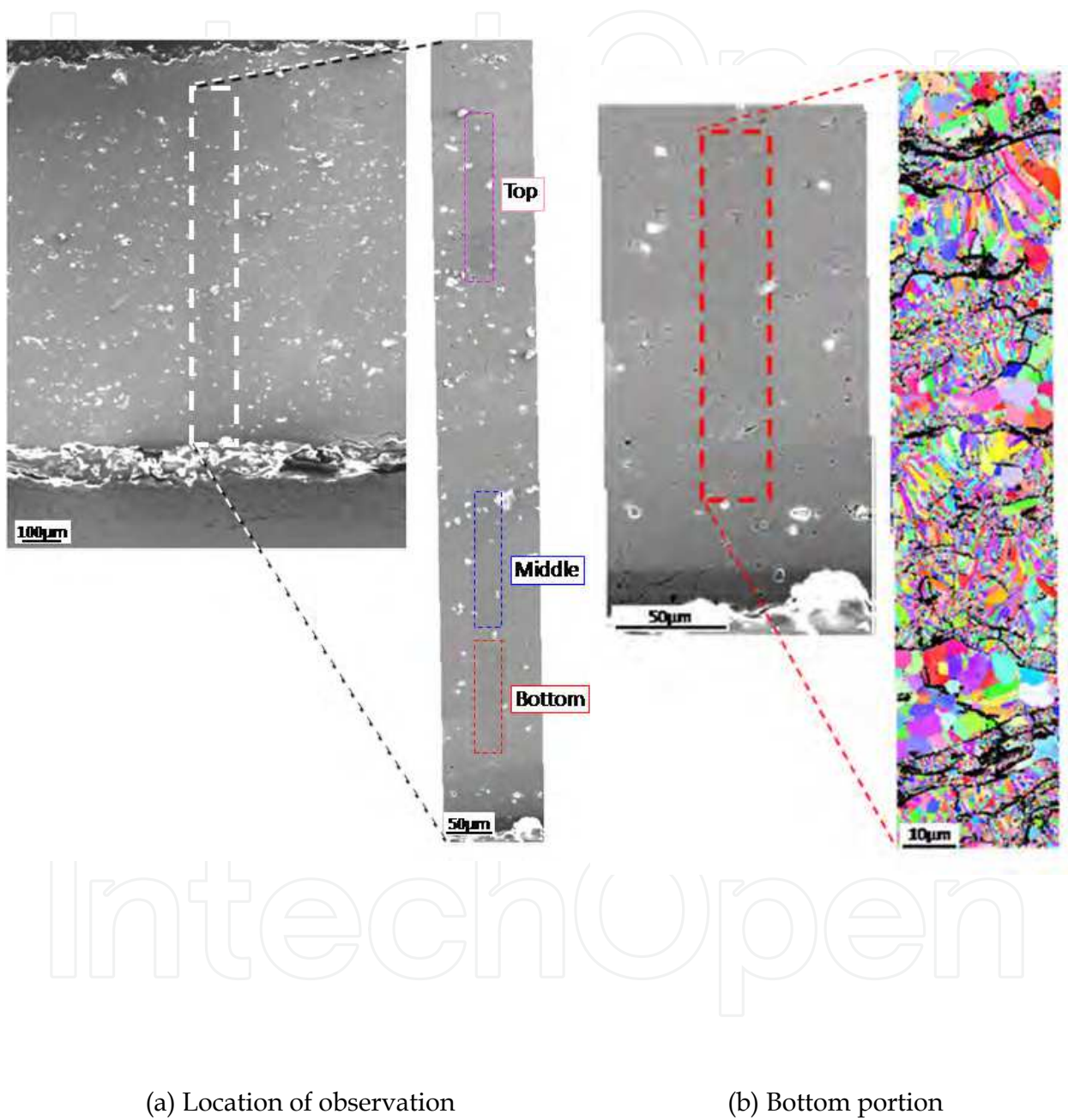


Fig. 9. Matching of IPF maps and SEM image for the sample exposed at 900°C for 500h.

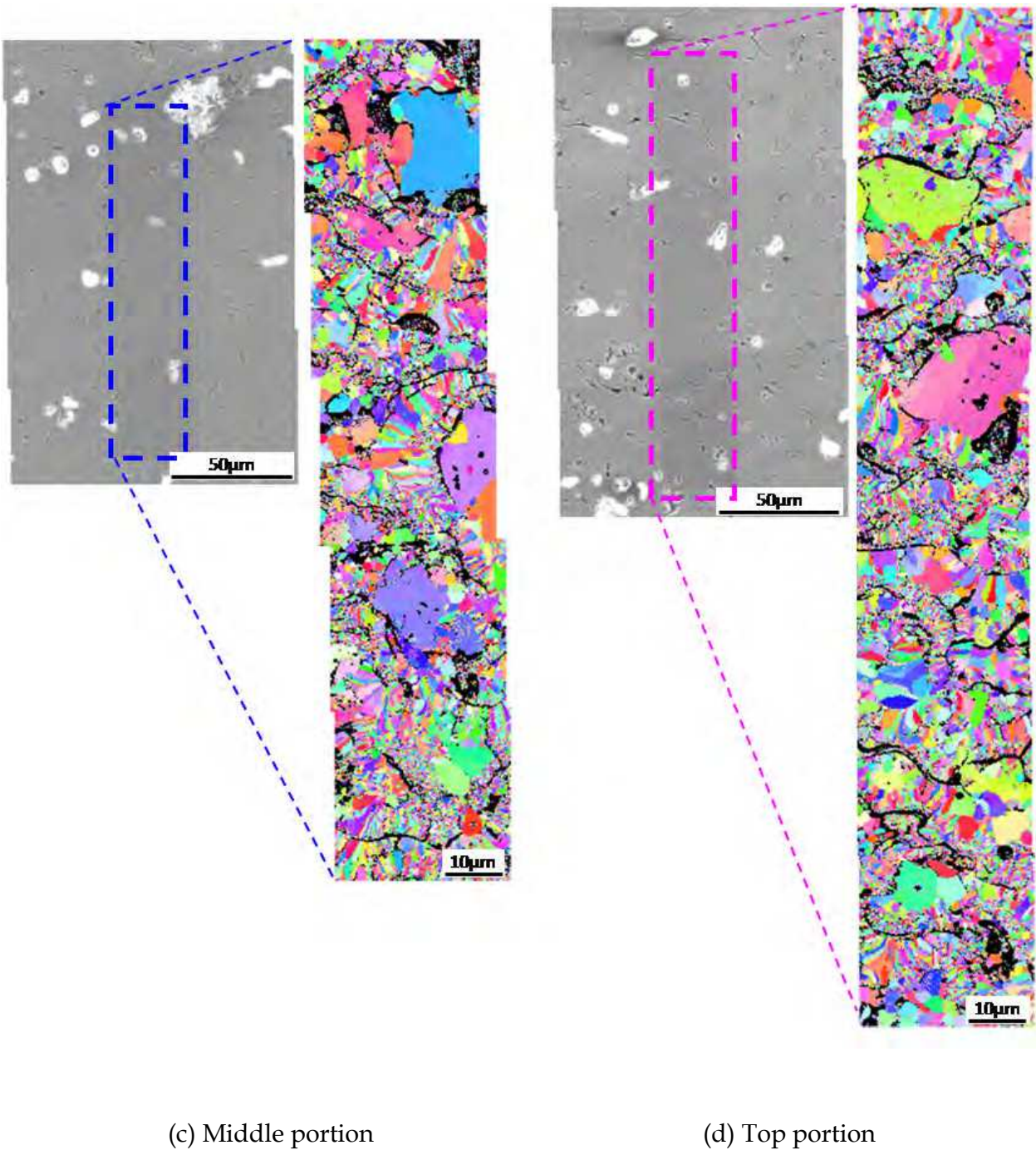


Fig. 9. Matching of IPF maps and SEM image for the sample exposed at 900°C for 500h (continued).

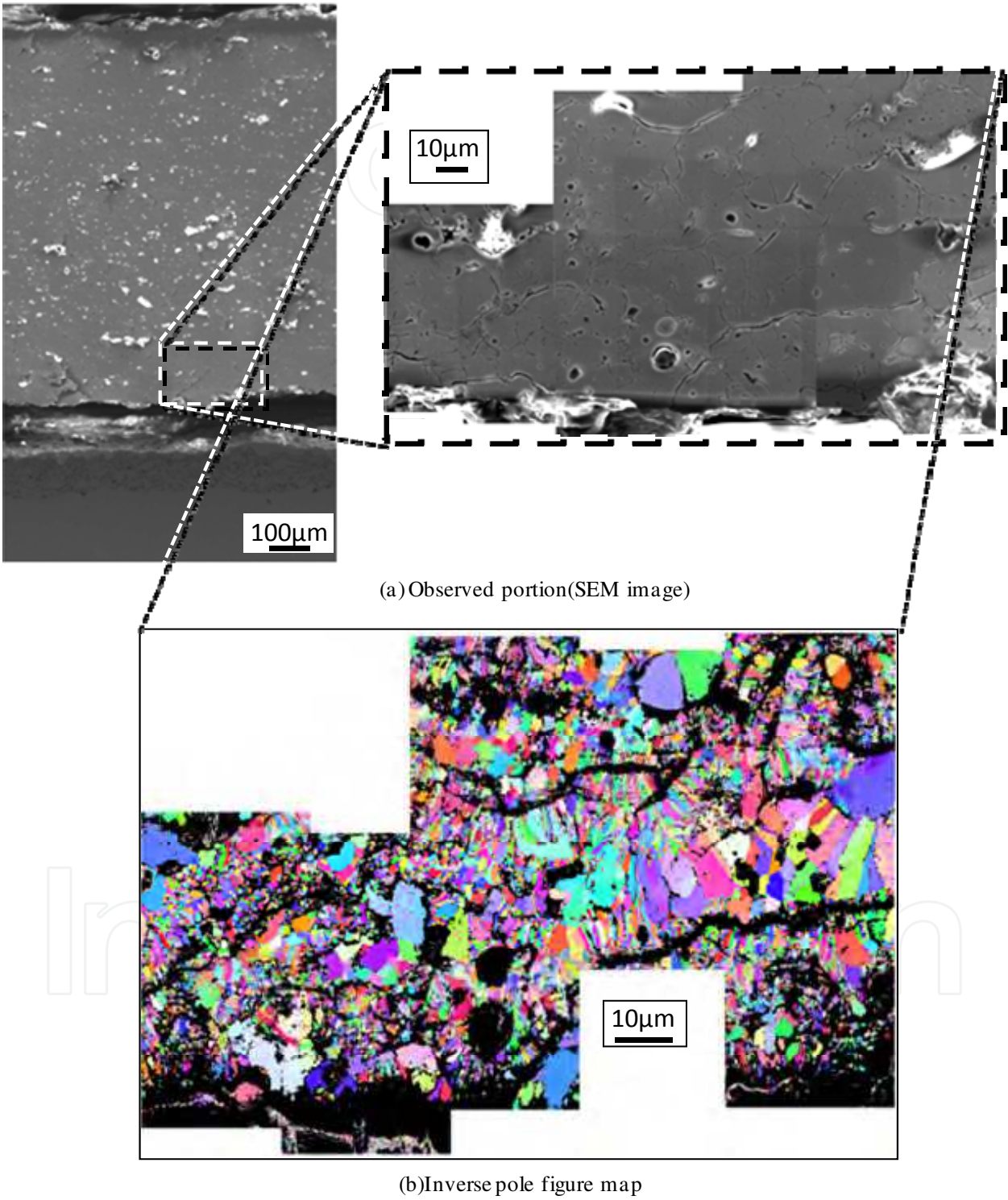


Fig. 10. Matching of SEM observations and IPF map of 1000°C-50h aged sample.

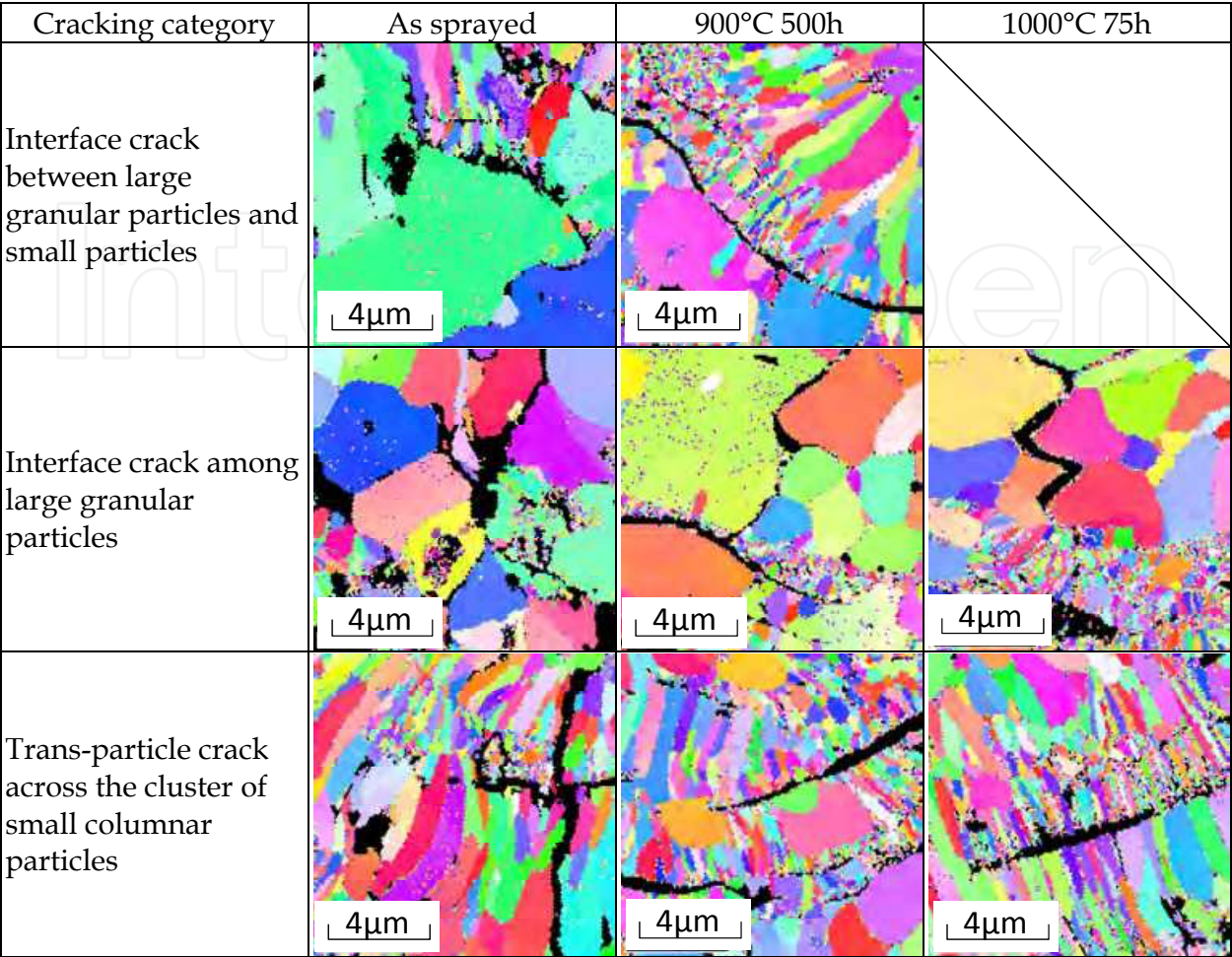
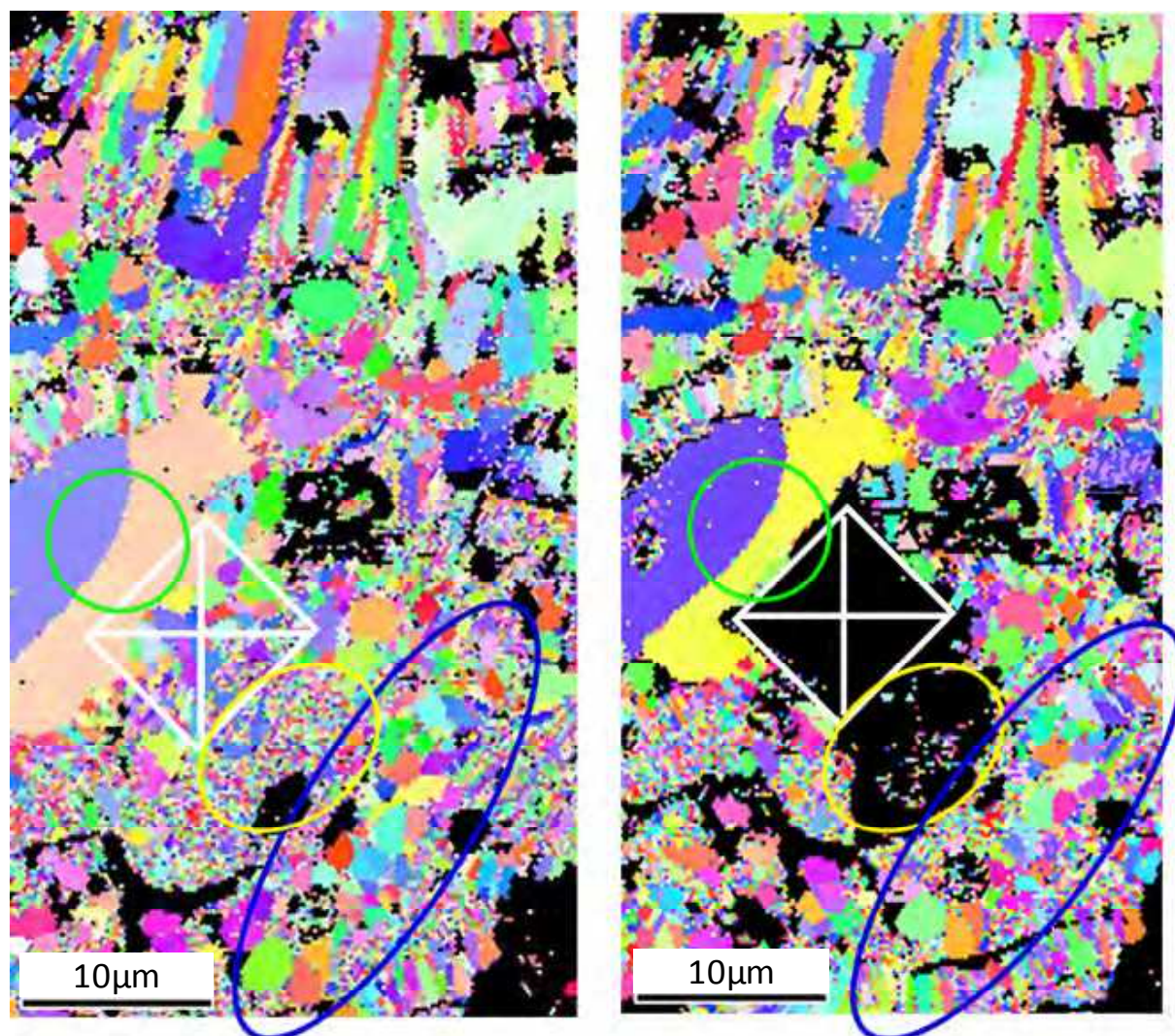


Fig. 11. Crack morphologies observed by IPF maps at top coat.

Figure 13 shows the IPF maps of heated sample at 1000°C/75hours before and after indentation test. The features of cracking showed no significant difference in the cracking morphologies with as sprayed samples shown in Fig.12. Fig.14 shows another view of IPF map with SEM image after indentation test for the same sample in Fig.13. The tendency of intergranular cracking in columnar particles is apparent but some cracks propagate across the particles. As a crack emanated from the bottom corner of the indentation is arrested at the splat boundary, the higher resistance for transgranular cracking than intergranular cracking is strongly suggested.

As demonstrated here, EBSD observation is proved to be a very powerful tool for identifying the crack morphologies and studying the resistance for cracking with respect to splat morphologies though further study is required to study precise crystal system and orientations.

Figure 16 shows the trace examples of micro cracks based on SEM observation in the top coat near bond coat region. The crack orientation is relatively random according to the splat morphologies as shown above. Crack growth may occur due to the coalescence of micro cracks which becomes more frequently at the later stage of exposure time. Crack length density is obtained as the ratio of total sum of crack length and the observed area.



(a) Before indentation test

(b) After indentation test

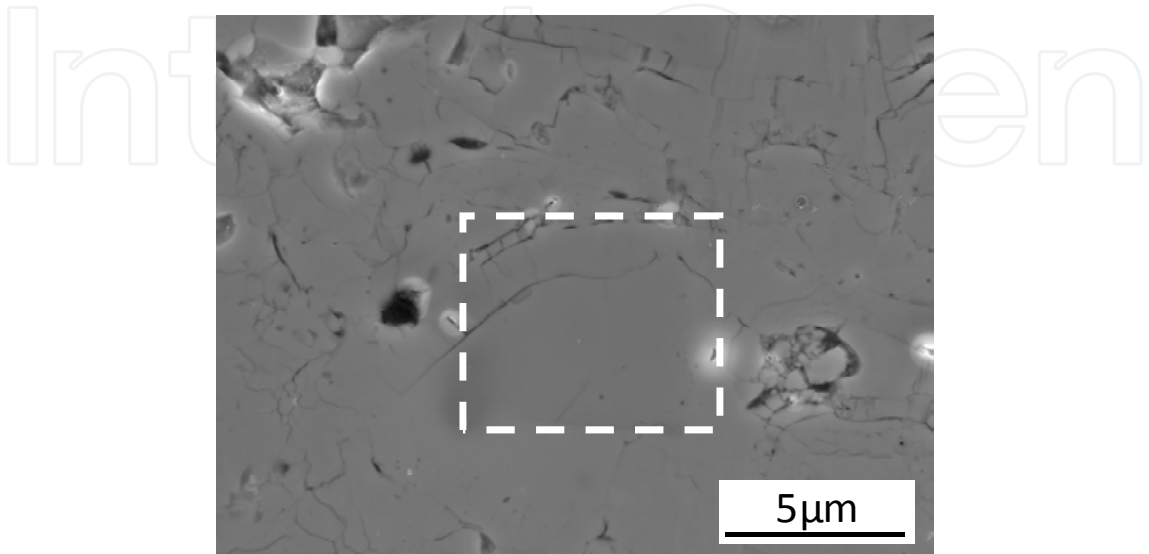
Fig. 12. IPF maps for as sprayed top coat sample before and after the indentation test.

Figure 17 shows the trend of crack length density against exposure time. Significant increase in crack length density was observed at the final stage of delamination for both exposure temperatures.

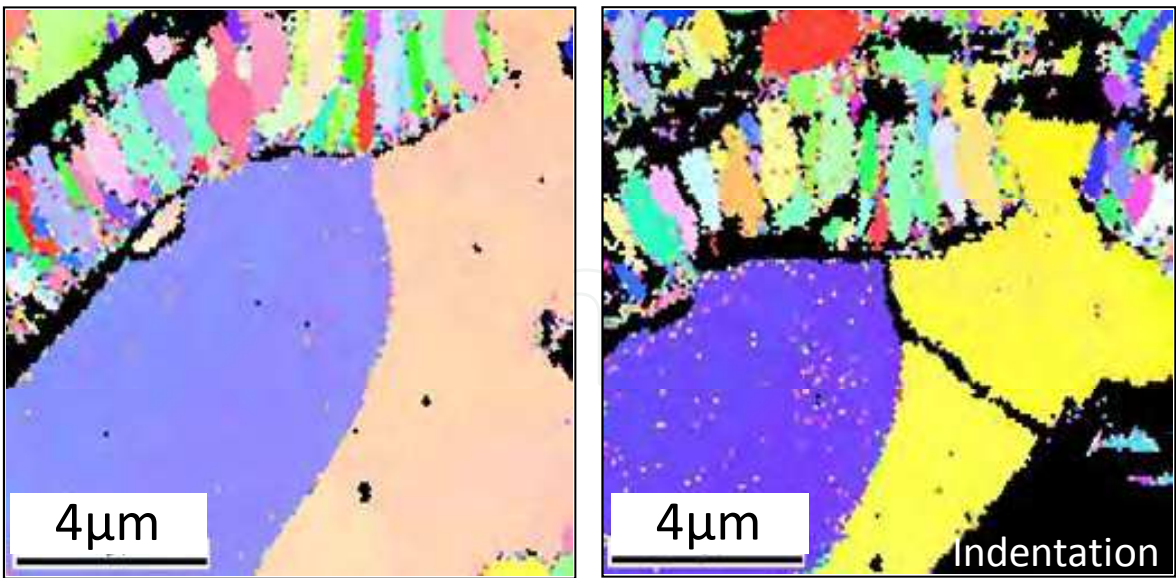
EDS analysis showed Al oxides and Cr oxides at TGO as shown in Fig.18. Cr oxides bulged toward top coat from TGO film consisted of Al oxides and enhancing top coat cracking. The initial significant increase and successive constant trend of TGO thickness was observed. The time to attain around 5% area percent of Cr oxide in TGO total area was corresponding to the intensive cracking in top coat. Thus, the Cr oxide growth enhanced the cracking of top coat strongly.

Figure 19 shows the trend of average TGO thickness against exposure time. The initial significant increase and successive constant trend of TGO thickness was observed for both exposure temperatures. Fig.20 shows the area fraction (%) of Al oxide and Cr oxide to total (Al + Cr) oxide area against exposure time. For Al oxide, the growth trend is almost similar

in both exposure temperatures but for Cr oxide the growth trend is quite different. The time to exceed 30% area fraction might corresponding to the onset of intensive cracking in top coat. Thus, the Cr oxide growth was thought to be an enhancing factor of cracking in top coat.



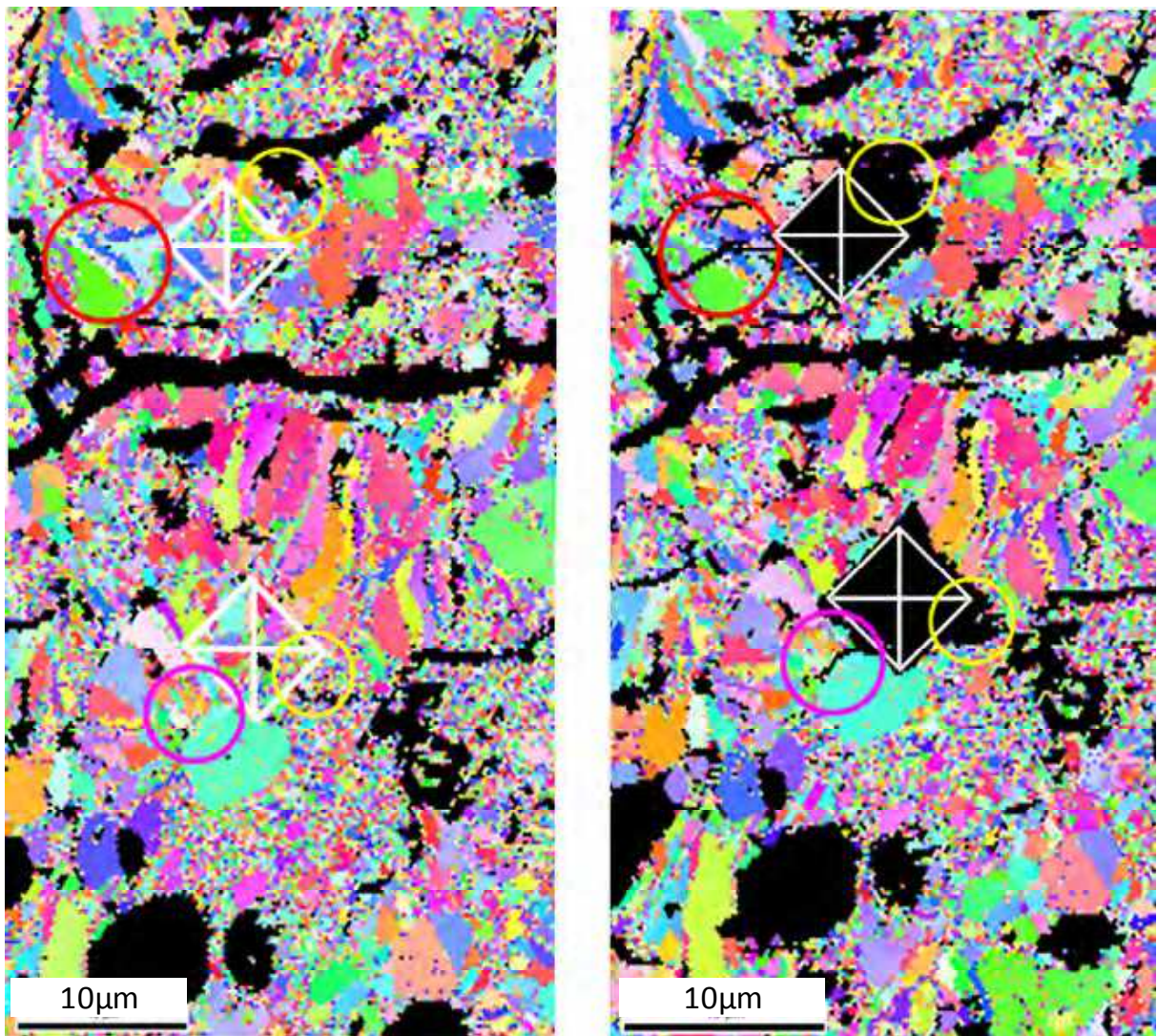
(a) Observation area in SEM image



(b) IPF map before indentation test

(c) IPF map after indentation test

Fig. 13. IPF maps for as sprayed top coat sample before and after the indentation test in higher magnification of Fig. 12.



(a) Before indentation test

(b) After indentation test

Fig. 14. IPF maps for 1000 °C -75h heated top coat samples before and after the indentation test.

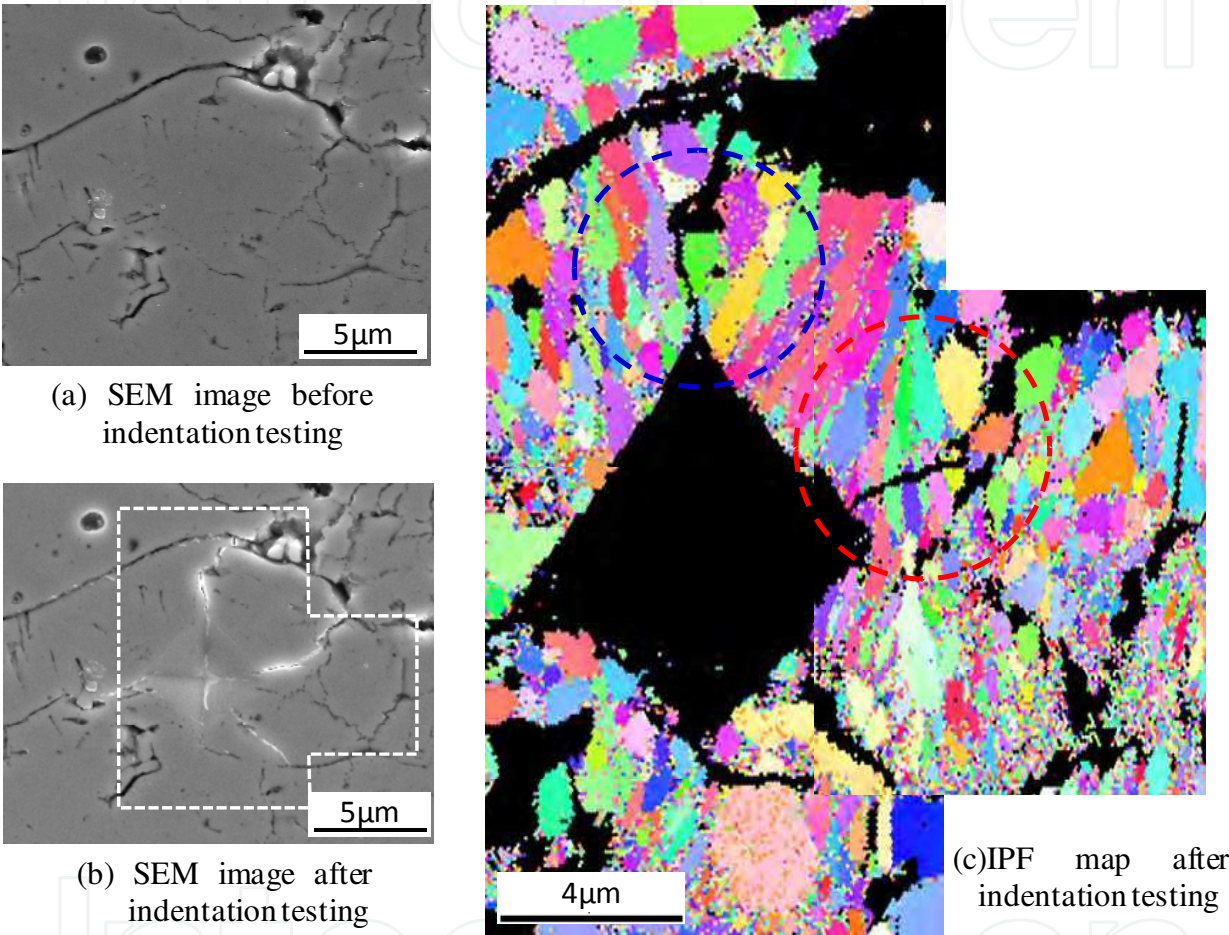


Fig. 15. Matching of SEM image and IPF map for 1000 °C -75h heated top coat samples before and after the indentation test.

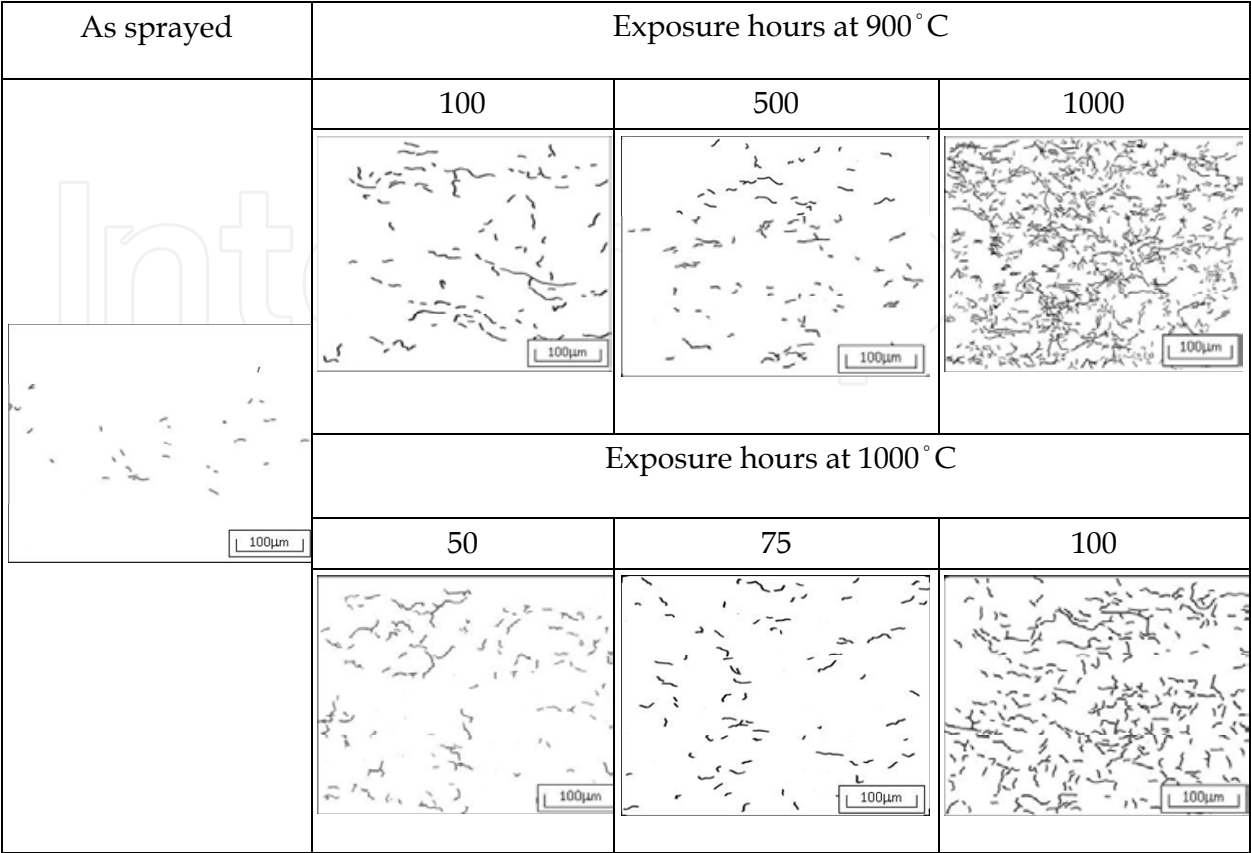


Fig. 16. Trace of cracks in top coat.

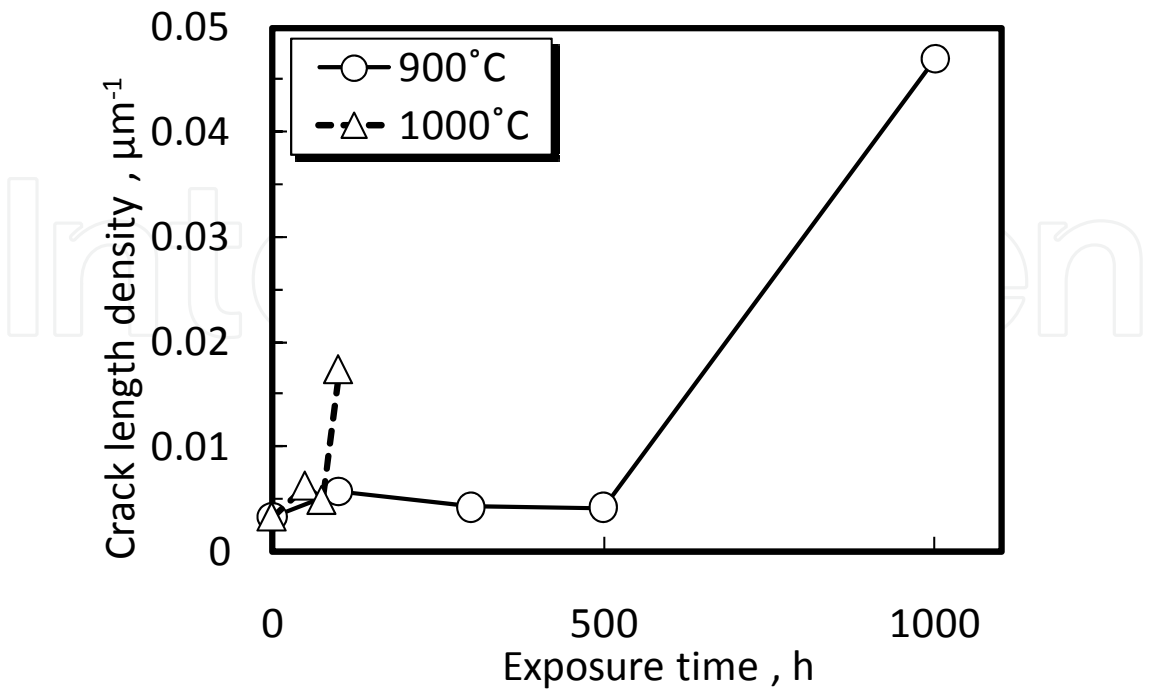


Fig. 17. Crack length density in top coat against exposure time.

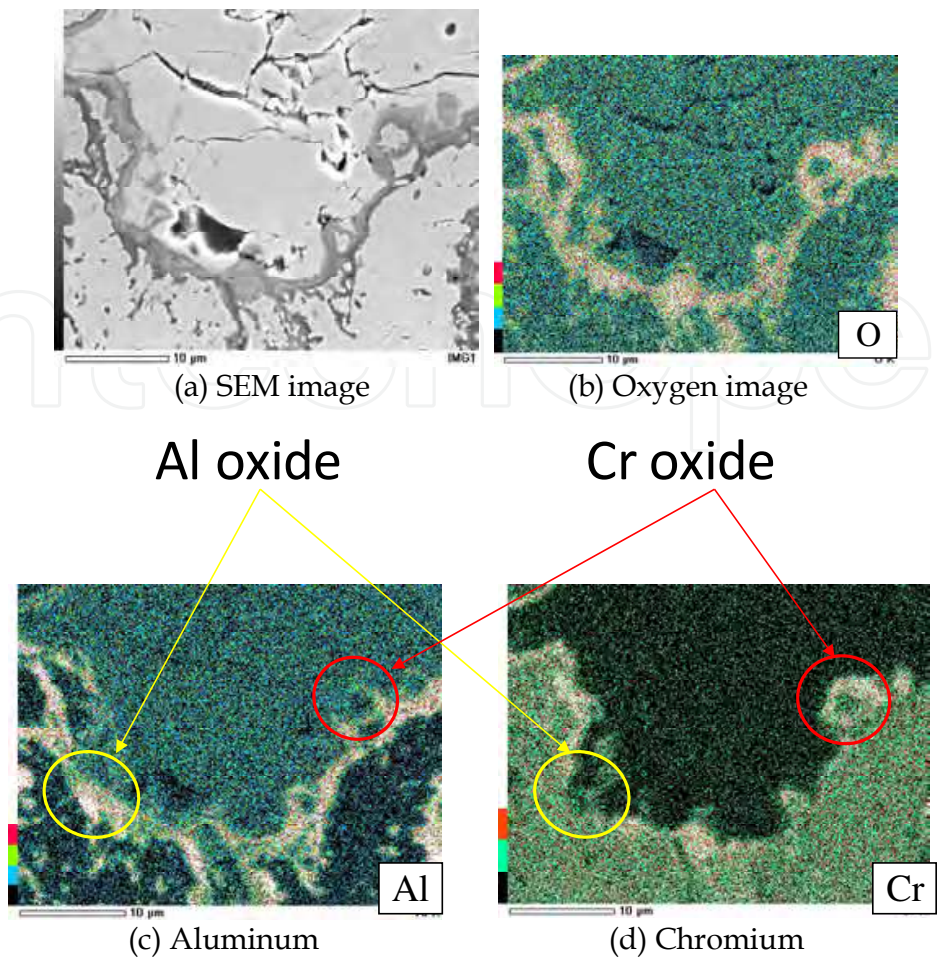


Fig. 18. Observation and element analysis of TGO.

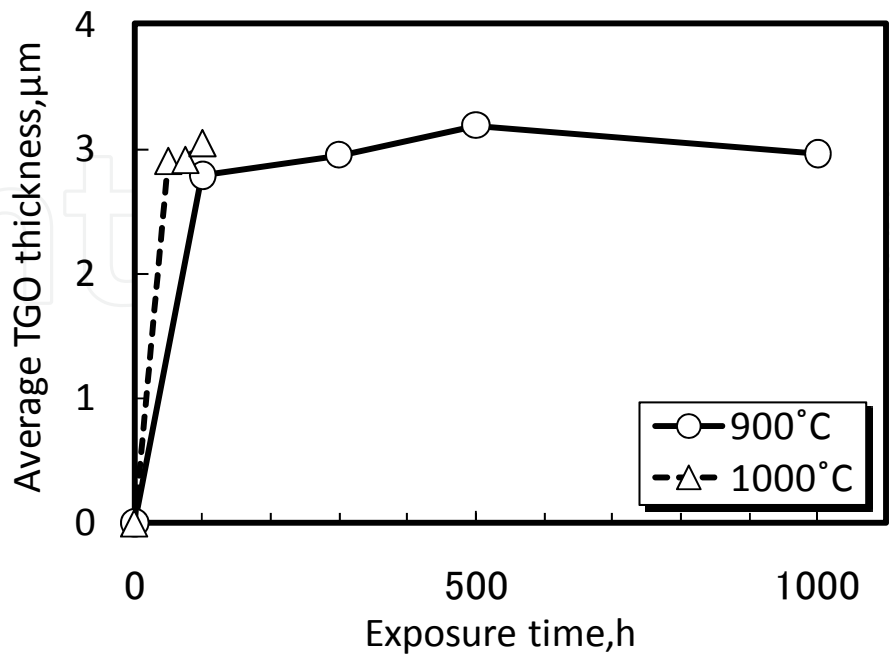


Fig. 19. Trend of average TGO thickness against exposure time.

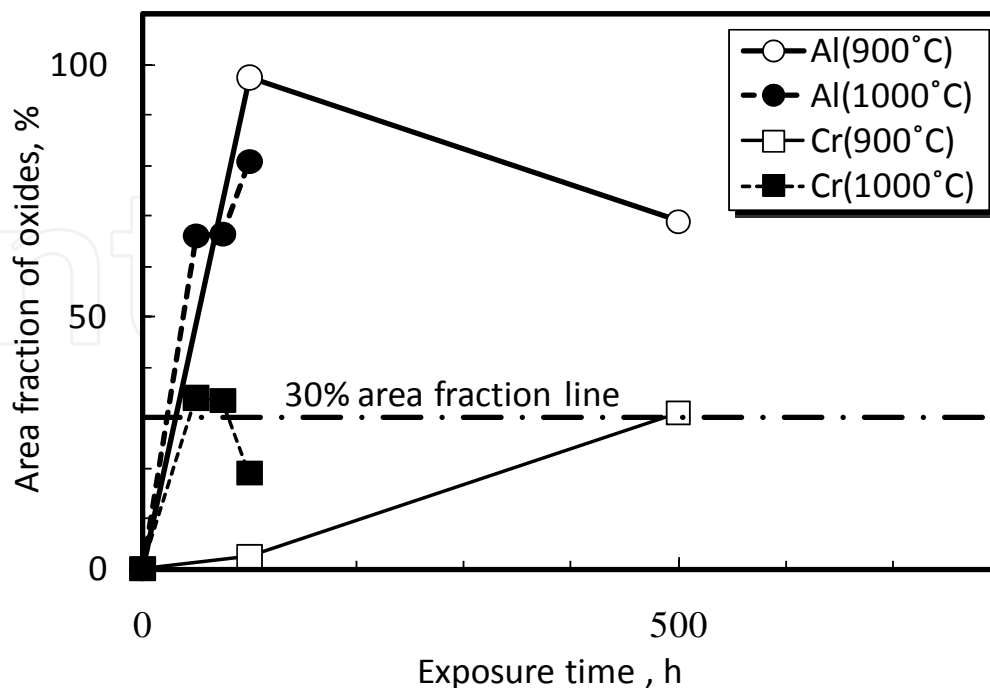


Fig. 20. Relationship between the area fraction of oxides and exposure time.

5. Summary

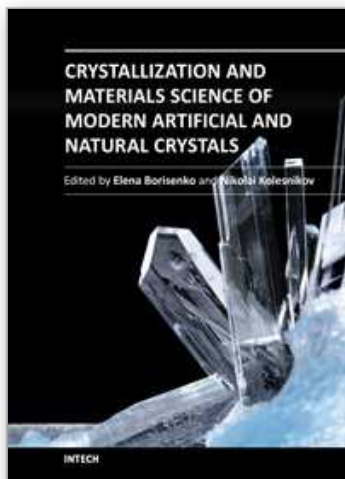
Microscopic and crystallographic observation techniques are very useful for investigating the damage and degradation process for structural materials. This article presented several results on the microstructural and crystallographic features during the heating process of TBC as follows.

1. Reduction of pores was observed by optical microscope observation due to thermal exposure and possibly attributed to the sintering of ceramics in top coat, though the reduction trend was not completely monotonic.
2. Micro cracking morphologies of top coat were divided into three typical patterns through EBSD observation: intergranular type along large splats, of interfacial type between large splats and the cluster of small columnar splats and of transgranular type across the cluster of small columnar splats.
3. The cracking were supposed to occur during cooling process after crystallization because the crack paths were strongly affected by particle morphologies and across the small columnar particles.
4. By indentation testing coupled with EBSD observation, the vulnerable spot of top coat to cracking and falling out were proved to be intergranular paths between relatively large splat particles and very small particle zones respectively.
5. The transition from small distributed cracking to large macro cracking was closely related to the Cr oxide formation toward top coat.

Further investigation should be conducted to reveal the effect of crystallographic characteristics on micro cracking in TBCs by upgrading EBSD analysis techniques for more precise crystalline system's identification and damage evaluation.

6. References

- [1] Okazaki, M., The Potential for the Improvement of High Performance Thermal Barrier Coatings (Review), *Material Science Research International*, Vol.9, No.1 (2003), pp.3-8.
- [2] Annigeri, R., DiMascio, P.S., Orenstein, R.M., Zuiker, J.R., Thompson, A.M., Lorraine, P.W. and Dubois, M., Life Assessment of Thermal Barrier Coatings for Gas Turbine Applications, *ASME 200-GT-580*, (2000), pp.1-8.
- [3] Wilkinson, A.J., Meaden, G. and Dingley, D.J., High Resolution Mapping of Strains and Rotations using Electron Backscatter Diffraction, *Materials Science and Technology*, Vol.22, No.11, (2006), pp.1271-1278.
- [4] Schwartz, A.J., Kumar, M., Adams, L.B., Field, D.P., *Electron Backscatter Diffraction in Materials Science*, Second Edition, Springer, (2009).
- [5] K. Fujiyama, H. Nakaseko, Y. Kato and H. Kimachi, EBSD Observation of Micro Crack Morphologies after Thermal Exposure in Thermal Barrier Coatings, *J. Solid Mechanics and Material Engineering*, JSME, Vol.4, No.2, (2010), pp.178-188.



Crystallization and Materials Science of Modern Artificial and Natural Crystals

Edited by Dr. Elena Borisenko

ISBN 978-953-307-608-9

Hard cover, 328 pages

Publisher InTech

Published online 20, January, 2012

Published in print edition January, 2012

Crystal growth is an important process, which forms the basis for a wide variety of natural phenomena and engineering developments. This book provides a unique opportunity for a reader to gain knowledge about various aspects of crystal growth from advanced inorganic materials to inorganic/organic composites, it unravels some problems of molecular crystallizations and shows advances in growth of pharmaceutical crystals, it tells about biomineralization of mollusks and cryoprotection of living cells, it gives a chance to learn about statistics of chiral asymmetry in crystal structure.

How to reference

In order to correctly reference this scholarly work, feel free to copy and paste the following:

Kazunari Fujiyama (2012). Crystallographic Observation and Delamination Damage Analyses for Thermal Barrier Coatings Under Thermal Exposure, Crystallization and Materials Science of Modern Artificial and Natural Crystals, Dr. Elena Borisenko (Ed.), ISBN: 978-953-307-608-9, InTech, Available from: <http://www.intechopen.com/books/crystallization-and-materials-science-of-modern-artificial-and-natural-crystals/crystallographic-observation-and-delamination-damage-analyses-for-thermal-barrier-coatings-under-the>

INTech
open science | open minds

InTech Europe

University Campus STeP Ri
Slavka Krautzeka 83/A
51000 Rijeka, Croatia
Phone: +385 (51) 770 447
Fax: +385 (51) 686 166
www.intechopen.com

InTech China

Unit 405, Office Block, Hotel Equatorial Shanghai
No.65, Yan An Road (West), Shanghai, 200040, China
中国上海市延安西路65号上海国际贵都大饭店办公楼405单元
Phone: +86-21-62489820
Fax: +86-21-62489821

© 2012 The Author(s). Licensee IntechOpen. This is an open access article distributed under the terms of the [Creative Commons Attribution 3.0 License](https://creativecommons.org/licenses/by/3.0/), which permits unrestricted use, distribution, and reproduction in any medium, provided the original work is properly cited.

IntechOpen

IntechOpen